Output-Positive Adaptive Control of Hyperbolic PDE-ODE Cascades

Ji Wang, *Member, IEEE*, and Miroslav Krstic, *Fellow, IEEE*

***Abstract*—In this article, we propose a new adaptive control barrier function (aCBF) method to design the output-positive adaptive control law for a hyperbolic PDE-ODE cascade with parametric uncertainties. This method employs the recent adaptive control approach with batch least-squares identification (BaLSI, pronounced "ballsy") that completes perfect parameter identification in finite time and offers a previously unforeseen advantage in safe control design with aCBF, which we elucidate in this article. Since the true challenge is exhibited for CBF of a high relative degree, we undertake a control design in this article for a class of systems that possess a particularly extreme relative degree: 2×2 hyperbolic PDEs sandwiched by a strict-feedback nonlinear ODE and a linear ODE, where the unknown coefficients are associated with the PDE in-domain coupling terms and with the input signal of the distal ODE. The designed output-positive adaptive controller guarantees the positivity of the output signal that is the furthermost state from the control input as well as the exponential regulation of the overall plant state to zero. The effectiveness of the proposed method is illustrated by numerical simulation.**

***Index Terms*—Adaptive control, backstepping, control barrier function, hyperbolic PDEs, least-squares identifier.**

I. Introduction

The safe control with adaptive control barrier function (aCBF), employing conventional continuous infinite-time adaptation, requires that the initial conditions be restricted to a subset of the safe set due to parametric uncertainty, where the safe set is shrunk in inverse proportion to the adaptation gain. The recent regulation-triggered adaptive control approach with batch least-squares identification (BaLSI, pronounced "ballsy") completes perfect parameter identification in finite time and offers a previously unforeseen advantage in aCBF-based safe control, which we elucidate in this article. We will present the control design based on a class of heterodirectional coupled hyperbolic PDEs [9], [27], physically motivated by control of delivery unmanned aerial vehicles with avoiding collision of hanging loads with the surrounding environment, as described in [30, Sec. A].

A. Control Barrier Functions

The positive-output control refers to keeping the system's output state within a safe region that is above the zero line. As is well known, one way to constrain the state in a safe region is the barrier Lyapunov function (BLF) method [26], [35], [36]. However, a major limitation of the BLF-based method is that while it ensures safety, it also enforces invariance of every level set, which makes it overly strong and conservative [3]. The control barrier functions (CBFs), introduced in [2], turn out to be a powerful tool for the safe control design, which is often accompanied by a quadratic program (QP) safety filter overriding a potentially unsafe nominal control signal to generate safe control actions. High relative degree CBFs were considered in the articles [23], [33], [34], following the introduction of a non-overshooting control design in [16] that is considered as the root of high-relative-degree CBF terminology. With the tools from [16], mean-square stabilization of stochastic nonlinear systems to an equilibrium at the barrier was solved in [18], and prescribed-time safety design which enforces safety only for a finite time of interest to the user was proposed in [1]. The above-mentioned safe control results focus on the systems described by ODEs. Very few results address CBF-based safe control for PDEs. The first one is presented in [14] for a Stefan PDE model with actuator dynamics, and the event-triggered version is further proposed in [13].

B. Adaptive Control Barrier Functions

In the presence of model uncertainties, most existing safety results with aCBFs are built upon the idea of aCLFs proposed in [17]. The pioneering and representative work of aCBFs is [25] which presents a variant of aCLFs in the context of safety: aCBFs, rendering the system solutions constrained to a subset of the original safe set. Some extensions made in [19] and also [21] alleviate the conservatism. Besides, Lopez and Slotine [20] permited the use of the certainty equivalence principle, simplifying the procedure in [19] and[25]. The development on adaptive safety with features of multiple CBFs [10] was made as well. Unlike the above-mentioned results, Wang and Xu [32] took into account the uncertainties in the control-input matrix. The aforementioned works focus only on adaptive safety, Cohen and Belta [8] made an attempt to synthesize adaptive safety and exponential stabilization. The above-mentioned aCBF-based safe adaptive control designs are for ODEs. To the best of our knowledge, this has not been pursued for PDEs. In this article, we make use of the batch least-squares identifier (BaLSI) adaptive scheme to propose a new aCBF method to design a safe adaptive controller for not only an ODE, but also a system consisting of PDEs and ODEs. The BaLSI was first proposed in [11] for nonlinear ODEs and then extended to PDEs in [12] and [28]. Unlike most least-squares estimation methods [5], [6], [7], [15], [31], where persistency of excitation (PE) is required to guarantee the parameter convergence, BaLSI does not require the PE assumption.

C. Main Contribution

1) This is the first result of aCBF-based safe adaptive PDE control. The previous PDE adaptive control designs [4], [12], [24] focus on the stabilization without dealing with safe constraints of the states. 2) As compared to the representative work on aCBF-based safe adaptive control [25], which requires that the initial conditions be restricted to a subset of the safe set and constrains the system solution to a subset of the original safe set due to parametric uncertainties, our safe adaptive control design does not impose extra restrictions on initial states beyond the safe set and maintains the states in the original safe region after a finite time.

Received 24 June 2024; revised 8 January 2025; accepted 6 May 2025. Date of publication 9 May 2025; date of current version 29 September 2025. This work was supported by the National Natural Science Foundation of China under Grant 62203372. Recommended by Associate Editor V. Andrieu. *(Corresponding author: Ji Wang.)*

Ji Wang is with the Department of Automation, Xiamen University, Xiamen 361005, China (e-mail: jiwang@xmu.edu.cn).

Miroslav Krstic is with the Department of Mechanical and Aerospace Engineering, University of California, San Diego, La Jolla, CA 92093 USA (e-mail: krstic@ucsd.edu).

Digital Object Identifier 10.1109/TAC.2025.3568557

D. Notation

1) The symbol $\mathbb{Z}_+$ denotes the set of all nonnegative integers, $\mathbb{N}$ denotes the set $\{1, 2, \cdots\}$, i.e., the natural numbers without 0, and $\mathbb{R}_+ := [0, +\infty)$.
2) Let $U \subseteq \mathbb{R}^n$ be a set with nonempty interior and let $\Omega \subseteq \mathbb{R}$ be a set. By $C^0(U; \Omega)$, we denote the class of continuous mappings on U, which takes values in Ω. By $C^k(U; \Omega)$, where $k \geq 1$, we denote the class of continuous functions on U, which have continuous derivatives of order k on U and take values in Ω.
3) We use the notation $L^2(0, 1)$ for the standard space of the equivalence class of square-integrable, measurable functions $f : (0, 1) \to \mathbb{R}$, with $\|f\|^2 := \int_0^1 f(x)^2 dx < +\infty$ for $f \in L^2(0, 1)$. For an integer $k \geq 1$, $H^k(0, 1)$ denotes the Sobolev space of functions in $L^2(0, 1)$ with all its weak derivatives up to order k in $L^2(0, 1)$.
4) Let $u : \mathbb{R}_+ \times [0, 1] \to \mathbb{R}$ be given. We use the notation $u[t]$ to denote the profile of u at certain $t \geq 0$, i.e., $u[t] = u(x, t)$ for all $x \in [0, 1]$.
5) The notation $f^{(i)}(t)$ denote i times derivatives of f. We use $\alpha_x^{(i)}(x, t)$ to denote i times derivatives with respect to x of $\alpha(x, t)$. Similarly, $\alpha_t^{(i)}(x, t)$ denote i times derivatives with respect to t of $\alpha(x, t)$.
6) Define $\underline{x}_j := [x_1, x_2, \ldots, x_j]^T$, and $\underline{\Gamma}^{(i)}(t) := [\Gamma^{(1)}(t), \Gamma^{(2)}(t), \ldots, \Gamma^{(i)}(t)]^T$.
7) Define C_i as a vector with ith entry as 1 and other entries are zero.

For ease of presentation, we omit or simplify the arguments of functions when no confusion arises. Besides, if $a > b$ happens in $\sum_{i=a}^b$ of this article, it means that the result is zero.

II. Problem Formulation

The considered plant is

$$\dot{Y}(t) = AY(t) + Bw(0, t) \tag{1}$$

$$z_t(x, t) = -q_1 z_x(x, t) + d_1 w(x, t) \tag{2}$$

$$w_t(x, t) = q_2 w_x(x, t) + d_2 z(x, t) \tag{3}$$

$$z(0, t) = pw(0, t) \tag{4}$$

$$w(1, t) = x_1(t) \tag{5}$$

$$\dot{x}_j(t) = x_{j+1}(t) + f_j(\underline{x}_j),\ j = 1, \ldots, m-1 \tag{6}$$

$$\dot{x}_m(t) = f_m(\underline{x}_m) + \sum_{i=0}^{m-1} \bar{q}_i z^{(i)}(1, t) + M^T Y(t) + U(t) \tag{7}$$

$\forall (x, t) \in [0, 1] \times [0, \infty)$, where $X^T(t) = [x_1, x_2, \ldots, x_m] \in \mathbb{R}^m$ and $Y^T(t) = [y_1, y_2, \ldots, y_n] \in \mathbb{R}^n$ are ODE states, the scalars $z(x, t) \in \mathbb{R}$, $w(x, t) \in \mathbb{R}$ are states of the PDEs. The function $U(t)$ is the control input to be designed. The actuator X-ODE is a strict-feedback nonlinear system, where the nonlinearities f_j satisfy Assumption 1. The Y-ODE (1) is a linear model, where the matrix A, the column vector B are in the form of $A = [0, 1, 0, 0, \ldots, 0; 0, 0, 1, 0, \ldots, 0; \cdots ; 0, 0, 0, 0, \ldots, 1; l_1, l_2, l_3, \ldots, l_{n-1}, l_n]_{n\times n}$ and $B = [0; 0; \cdots ; 0; b]_{n\times 1}$ with arbitrary constants $l_1, l_2, l_3, \ldots, l_{n-1}, l_n$, and $b > 0$ (without any loss of generality for $b < 0$). This indicates that the Y-ODE is in the controllable form that covers many practical models. Other plant parameters in (2)–(7), i.e., $d_1, d_2, p, q, \bar{q}_i, i = 0, \ldots, m-1$, and $q_1 > 0, q_2 > 0$ that denote the transport speed, as well as the n-dimensional row vector M^T, are also arbitrary. The parameter b that exists in the distal ODE, and the coefficients d_1, d_2 of the PDE in-domain couplings that are the potentially destabilizing terms are unknown. The unknown parameters d_1, d_2, b satisfy Assumption 2. **Control objective**: To exponentially regulate the overall system, including the plant w-PDE, z-PDE, Y-ODE, and X-ODE, and enforce **"safety," defined here as the nonnegativity** (without any loss of generality for not exceeding a nonzero setpoint) **of the output** of the distal ODE, i.e., the state furthest from the control input: $y_1(t) \geq 0$, $\forall t \in [0, \infty)$. This means that the safe region is the one above the zero line.

Assumption 1: The functions f_j are $m - j$ times differentiable, and $f_j(\mathbf{0}) = 0$.

Assumption 2: The bounds of the unknown parameters d_1, d_2, b are known and arbitrary, i.e., $\underline{d}_1 \leq d_1 \leq \overline{d}_1, \underline{d}_2 \leq d_2 \leq \overline{d}_2, 0 < \underline{b} \leq b \leq \overline{b}$.

During the time interval $[0, \frac{1}{q_2}]$ no control action can reach the $Y(t)$ ODE due to the w-transport PDE. Therefore, we have to impose constrains on the initial states to ensure that the output $y_1(t) = C_1 Y(t)$ stays in the safe region before the control action begins to regulate the $Y(t)$-ODE.

Assumption 3: The initial values of the ODE and PDE states satisfy i) $y_1(0) \geq 0$; ii) $\Pi(\varsigma) = C_1 e^{A\frac{\varsigma}{q_2}} Y(0) + C_1 \frac{1}{q_2} e^{A\frac{\varsigma}{q_2}} \int_0^\varsigma e^{-A\frac{x}{q_2}} B(w(x, 0) - \int_0^x F(x, y) z(y, 0) dy - \int_0^x H(x, y) w(y, 0) dy) dx \geq 0$ for $0 < \varsigma < 1$ and $\Pi(1) > 0$, where the explicit expressions of $F(x, y)$ and $H(x, y)$ are given in [30, (B.7), (B.8)].

In Assumption 3, the condition i) implies there is no additional restriction on $y_1(0)$ but the original safe set; the condition ii) is the sufficient and necessary condition of $y_1(t) \geq 0$ on $t \in (0, \frac{1}{q_2})$ and $y_1(\frac{1}{q_2}) > 0$, i.e., before the control action begins to regulate the $Y(t)$-ODE, which will be proven in Lemma 1 latter. Besides, the following assumption on the actuator state makes the control action for Y-ODE begin within the region of safe regulation.

Assumption 4: The initial value of the actuator state $x_1(0)$ satisfies $x_1(0) > \int_0^1 \Psi(1, y) z(y, 0) dy + \int_0^1 \Phi(1, y) w(y, 0) dy + \lambda(1) Y(0)$, where explicit $\Psi(1, y)$, $\Phi(1, y)$, $\lambda(1)$ are given by [30, (A.9), (B.3), (B.9), (B.10)].

III. Nominal Output-Positive Control Design

A. First Nonundershooting Backstepping Transformation

Following [16], we apply the transformation

$$z_i(t) = y_i(t) - g_{i-1}(\underline{y}_{i-1}(t)),\ i = 1, \ldots, n \tag{8}$$

$$g_0 = 0 \tag{9}$$

$$g_i(\underline{y}_i(t)) = -\kappa_i z_i(t) + \sum_{j=1}^{i-1} \frac{\partial g_{i-1}}{\partial y_j} y_{j+1},\ i = 1, \ldots, n-1 \tag{10}$$

where the positive design parameters κ_i, $i = 1, \ldots, n$ are to be determined later, to convert the distal Y-ODE (1) into

$$\dot{Z}(t) = A_z Z(t) + Bw(0, t) - BK^T Y(t) \tag{11}$$

where $A_z = [-\kappa_1, 1, 0, 0, \ldots, 0, 0;\ 0, -\kappa_2, 1, 0, \ldots, 0, 0; \cdots ; 0, 0, 0, 0, \ldots, -\kappa_{n-1}, 1; 0, 0, 0, \ldots, 0, 0, -\kappa_n]_{n\times n}$ is Hurwitz, and the constant row vector

$$K^T = \frac{1}{b}\Bigg[-l_1 + \kappa_n \frac{\partial g_{n-1}}{\partial y_1}, -l_2 + \frac{\partial g_{n-1}}{\partial y_1} + \kappa_n \frac{\partial g_{n-1}}{\partial y_2}, \ldots, -l_{n-1} + \frac{\partial g_{n-1}}{\partial y_{n-2}} + \kappa_n \frac{\partial g_{n-1}}{\partial y_{n-1}}, -l_n + \frac{\partial g_{n-1}}{\partial y_{n-1}} - \kappa_n\Bigg]_{1\times n}. \tag{12}$$

Note: if $n = 1$, then K in (12) is equal to $-l_1 - \kappa_1$, i.e., inserting $n = 1$ into the last term in (12) with recalling $g_0 = 0$. Similarly, if $n = 2$, then K is a 2-D vector consisting of the first and last terms in (12). Considering the linear system (1), $g_{n-1}(\underline{y}_{n-1}(t))$ can be expressed as a linear combination of y_i, $i = 1, \ldots, n-1$, i.e., $g_{n-1}(\underline{y}_{n-1}(t)) = \sum_{i=1}^{n-1} \frac{\partial g_{n-1}}{\partial y_i} y_i$, where $\frac{\partial g_{n-1}}{\partial y_i}$ are constant. This fact has been used in deriving (12).

To achieve the original safety goal, the transformed states $Z(t) = [z_1, \ldots, z_n]^T$ need to be kept nonnegative on $t \in [\frac{1}{q_2}, \infty)$ (there is no control action for the distal ODE until $t = \frac{1}{q_2}$ because of the information transportation along the first-order hyperbolic PDEs).

B. Second PDE Backstepping Transformation

In order to remove the in-domain coupling destabilizing terms from the 2×2 hyperbolic PDE system and compensate the term $BK^TY(t)$ in (11), we introduce the following backstepping transformation [22]:

$$\alpha(x,t) = z(x,t) - \int_0^x \phi(x,y) z(y,t) dy - \int_0^x \varphi(x,y) w(y,t) dy - \gamma(x) Y(t) \tag{13}$$

$$\beta(x,t) = w(x,t) - \int_0^x \Psi(x,y) z(y,t) dy - \int_0^x \Phi(x,y) w(y,t) dy - \lambda(x) Y(t) \tag{14}$$

where $\phi, \varphi, \gamma, \Psi, \Phi, \lambda$ are defined in [30, Appendix A1]. The function $\beta(x,t)$ should be ensured nonnegative (for $t \in [\frac{1}{q_2}, \infty) \times x \in [0,1]$) in pursuing the original safety goal.

By (13), (14), the system (2)–(5) with (11) is converted into

$$\dot{Z}(t) = A_z Z(t) + B\beta(0,t) \tag{15}$$

$$\alpha(0,t) = p\beta(0,t) \tag{16}$$

$$\alpha_t(x,t) = -q_1 \alpha_x(x,t) \tag{17}$$

$$\beta_t(x,t) = q_2 \beta_x(x,t) \tag{18}$$

$$\beta(1,t) = x_1(t) - \Gamma(t) \tag{19}$$

where $\Gamma(t) = \int_0^1 \Psi(1,y) z(y,t) dy + \int_0^1 \Phi(1,y) w(y,t) dy + \lambda(1) Y(t)$.

C. Third Nonundershooting Backstepping Transformation

Similar to Section III-A, we introduce the following modified backstepping transformations for proximal X-ODE

$$h_i(t) = x_i(t) - \tau_{i-1} - \Gamma^{(i-1)}(t),\ i = 1, \ldots, m \tag{20}$$

$$\tau_0 = 0 \tag{21}$$

$$\tau_i(\underline{x}_i(t), \underline{\Gamma}^{(i-1)}(t)) = -c_i h_i(t) - f_i(\underline{x}_i(t)) + \sum_{j=1}^{i-1} \left[\frac{\partial \tau_{i-1}}{\partial x_j} (x_{j+1} + f_j(\underline{x}_j(t))) + \frac{\partial \tau_{i-1}}{\partial \Gamma^{(j-1)}(t)} \Gamma^{(j)}(t) \right]$$
$$i = 1, \ldots, m-1 \tag{22}$$

where the transformed states $h_i(t)$ of the proximal ODE also need to be kept nonnegative for all time to achieve the original safety goal. The positive constants $c_1, \ldots, c_m$ are design parameters whose conditions will be shown in the next section. According to $\Gamma(t)$ shown below (19), $\Gamma^{(i)}(t)$ is obtained as $\Gamma^{(i)}(t) = -\sum_{j=0}^{j=i-1} q_1 R_{i-1-j}(1) z_t^{(j)}(1,t) + \sum_{j=0}^{j=i-1} q_1 R_{i-1-j}(0) z_t^{(j)}(0,t) + \int_0^1 R_i(y) z(y,t) dy + \sum_{j=0}^{j=i-1} q_2 P_{i-1-j}(1) w_t^{(j)}(1,t) - \sum_{j=0}^{j=i-1} (q_2 P_{i-1-j}(0) - \lambda(1) A^{i-1-j} B) w_t^{(j)}(0,t) + \int_0^1 P_i(y) w(y,t) dy + \lambda(1) A^i Y(t)$, $i = 1, \ldots, m$ where the functions R_i, P_i are defined by $R_i(y) = q_1 R'_{i-1}(y) + d_2 P_{i-1}(y)$, $P_i(y) = -q_2 P'_{i-1}(y) + d_1 R_{i-1}(y)$, $i = 1, \ldots, m$, $R_0(y) = \Psi(1,y)$, $P_0(y) = \Phi(1,y)$ with the explicit solutions of $\Psi(1,y)$ and $\Phi(1,y)$ given by [30, (B.9), (B.10), (B.3), (B.7), (B.8)]. Please note that the m order derivatives of $\Psi(1,y)$ and $\Phi(1,y)$ exist according to Theorem 5 in [27].

Through the transformations (8)–(10), (13), (14), (20)–(22), now we convert the original system (1)–(7) to the target system consisting of (15)–(18) together with

$$\beta(1,t) = h_1(t) \tag{23}$$

$$\dot{h}_i(t) = -c_i h_i(t) + h_{i+1}(t),\ i = 1, \ldots, m-1 \tag{24}$$

$$\dot{h}_m(t) = -c_m h_m(t) \tag{25}$$

by choosing the control input as

$$U(t) = \tau_m - \sum_{i=0}^{m-1} \bar{q}_i z_t^{(i)}(1,t) - M^T Y(t) + \Gamma^{(m)}(t) := \mathcal{U}(\chi(t); \theta) \tag{26}$$

where $\chi(t)$, which denotes all the system signals used in the control law, can be written as $\chi(t) = [x_1(t), \ldots, x_m(t), w(0,t), \ldots, w_t^{(m-1)}(0,t), z(1,t), \cdots, z_t^{(m-1)}(1,t), \int_0^1 \mathcal{R}(x) w(x,t) dx, \int_0^1 \mathcal{P}(x) z(x,t) dx, y_1(t), \ldots, y_n(t)]$, for some $\mathcal{R}(x), \mathcal{P}(x)$ consisting of $R_i(x), P_i(x)$ defined in [30, (27)–(29)]. Writing $\theta = [d_1, d_2, b]^T$ after ";" in $\mathcal{U}(\chi(t); \theta)$ emphasizes the fact that the control law depends on the unknown parameters d_1, d_2, b. The calculation details in the third transformation are shown in [30, Appendix C].

D. Selection of Nonundershooting Design Parameters

We choose the design parameters $\kappa_1, \ldots, \kappa_{n-1}$ ($\kappa_n > 0$ is free) to satisfy

$$\kappa_i > \frac{\left(\sum_{j=1}^{i-1} \frac{\partial g_{i-1}}{\partial y_j} C_{j+1} - C_{i+1} \right) Y(\frac{1}{q_2})}{C_i Y\left(\frac{1}{q_2}\right) - g_{i-1}\left(\underline{C}_{i-1} Y\left(\frac{1}{q_2}\right)\right)} := \check{\kappa}_i(b) \tag{27}$$

for $i = 1, \ldots, n-1$, which includes the unknown parameter b, where $Y(\frac{1}{q_2})$ is expressed as the initial values of z-PDE, w-PDE, and Y-ODE as $Y\left(\frac{1}{q_2}\right) = e^{A\frac{1}{q_2}} Y(0) + \int_0^{\frac{1}{q_2}} e^{A(\frac{1}{q_2} - \tau)} B(w(q_2\tau, 0) - \int_0^{q_2\tau} F(q_2\tau, y) z(y,0) dy - \int_0^{q_2\tau} H(q_2\tau, y) w(y,0) dy) d\tau$, which can be seen clearly in the proof of [30, Lemma 1]. The expressions of $F(x,y)$ and $H(x,y)$ are given in [30, (B.7), (B.8)]. The purpose of choosing the design parameters as (27) is to make CBFs $z_i(t)$, $i = 2, \ldots, n$, positive at the time $t = \frac{1}{q_2}$ when the control action reaches the distal ODE, which will be shown in the next section.

The design parameters $c_1, \ldots, c_m$ are selected as

$$c_i > \max\{2, \check{c}_i(\theta)\},\ i = 1, \ldots, m-1,\ c_m > 1 \tag{28}$$

where

$$\check{c}_i(\theta) = \frac{1}{x_i(0) - \tau_{i-1}(\underline{x}_{i-1}(0), \underline{\Gamma}^{(i-2)}(0)) - \Gamma^{(i-1)}(0)} \times \Bigg[-x_{i+1}(0) - f_i(\underline{x}_i(0)) + \sum_{j=1}^{i-1} \Bigg[\frac{\partial \tau_{i-1}(\underline{x}_{i-1}(0), \underline{\Gamma}^{(i-2)}(0))}{\partial x_j(0)} (x_{j+1}(0) + f_j(\underline{x}_j(0))$$

$$+\frac{\partial\tau_{i-1}(\underline{x}_{i-1}(0),\underline{\Gamma}^{(i-2)}(0))}{\partial\Gamma^{(j-1)}(0)}\Gamma^{(j)}(0)\Bigg]+\Gamma^{(i)}(0)\Bigg] \tag{29}$$

for $i=1,\ldots,m-1$, which includes the unknown parameters $\theta=[d_1,d_2,b]^T$. The purpose of choosing the design parameters as (28) is to make CBFs $h_i(t)$, $i=2,\ldots,m$, positive at $t=0$ and ensure the stability through the Lyapunov analysis, which will be shown in the next section as well.

E. Result With Nominal Output-Positive Control

For the time interval $[0,\frac{1}{q_2}]$, no control action reaches the distal $Y(t)$-ODE, whose safety is ensured under the given initial conditions, which is shown in the following lemma.

Lemma 1: For the time period no control action reaches the Y-ODE, $y_1(t)$ is kept in the safe region, i.e., $y_1(t)\geq 0$, $t\in[0,\frac{1}{q_2})$ and $y_1(\frac{1}{q_2})>0$ under Assumption 3 regarding the initial data.

Proof: Please see the proof of [30, Lemma 1]. □

Next, we present two lemmas regarding initializing positively the CBFs $z_i(t)$, $h_i(t)$ of distal and proximal ODEs, at $t=\frac{1}{q_2}$ and $t=0$, by the selection of the design parameters κ_i and c_i in Section III-D, respectively.

Lemma 2: The positivity of $z_i(\frac{1}{q_2})$, i.e., the values of high-relative-degree ODE CBFs z_i at the time instant when the control action reaches the distal ODE, is ensured, i.e., $z_i(\frac{1}{q_2})>0$, $i=1,\ldots,n$, under the design parameters κ_i, $i=1,\ldots,n-1$ satisfying (27).

Proof: Recalling (8), (9), and Lemma 1, we know the base case $z_1(\frac{1}{q_2})=y_1(\frac{1}{q_2})>0$. We then show the induction step: if $z_i(\frac{1}{q_2})>0$, then $z_{i+1}(\frac{1}{q_2})>0$ under the choices of κ_i in (27) for $i=1,\ldots,n-1$. We obtain the expression of $z_{i+1}(\frac{1}{q_2})$ according to (8), (10). Recalling (27) where the denominator $C_iY(\frac{1}{q_2})-g_{i-1}(\underline{C}_{i-1}Y(\frac{1}{q_2}))=y_i(\frac{1}{q_2})-g_{i-1}(\underline{y}_{i-1}(\frac{1}{q_2}))=z_i(\frac{1}{q_2})>0$ which is obtained from the inductive hypothesis $z_i(\frac{1}{q_2})>0$, we have that $z_{i+1}(\frac{1}{q_2})>0$. Considering the base case and the induction step proved previously, this lemma is obtained. Due to the space limit, we only provide the sketch here. Please see the proof of [30, Lemma 2] for details. □

Lemma 3: The high-relative-degree ODE CBFs h_i are initialized positively, i.e., $h_i(0)>0$, $i=1,\ldots,m$, under the design parameters c_i, $i=1,\ldots,m-1$ satisfying (28).

Proof: It is similar to the proof of Lemma 2. Please see the proof of [30, Lemma 3] for details. □

The above-mentioned three lemmas will be used to prove the safety property stated in the following theorem.

Theorem 1: For initial data $w[0]\in C^{m-1}([0,1])$, $z[0]\in C^{m-1}([0,1])$, $X(0)\in\mathbb{R}^m$, $Y(0)\in\mathbb{R}^n$ satisfying Assumptions 1, 3, 4, for design parameters c_i, $i=1,\ldots,m$ satisfying (28) and κ_i, $i=1,\ldots,n-1$ satisfying (27), the closed-loop system including the plant (1)–(7) with the nominal safe controller (26) has the following properties.

1) Safety (output positivity) is ensured in the sense that $y_1(t)\geq 0$, $\forall t\geq 0$.
2) Exponential regulation is achieved in the sense that $\|w(\cdot,t)\|^2+\|z(\cdot,t)\|^2+|X(t)|^2+|Y(t)|^2$ is exponentially convergent to zero.
3) The control input is convergent to zero, i.e., $\lim_{t\to\infty}U(t)=0$.

Proof:

1) For the target system (15)–(18), (23)–(25), recalling the choice of the design parameters c_i (28) that makes CBFs $h_i(t)$, $i=2,\ldots,m$, positive at $t=0$ as shown in Lemma 3, and the choice of the design parameters κ_j (27) that makes CBFs $z_i(t)$, $i=2,\ldots,n$, positive at the time $t=\frac{1}{q_2}$ as shown in Lemma 2, we obtain the nonnegativity of CBFs: $h_i(t)\geq 0$, $i=1,\ldots,m$, on $t\in[0,\infty)$, $z_i(t)\geq 0$, $i=1,\ldots,n$ and $\beta(\cdot,t)\geq 0$ on $t\in[\frac{1}{q_2},\infty)$. As a result, $y_1(t)=z_1(t)>0$ for $t\in[\frac{1}{q_2},\infty)$. Recalling the fact that $y_1(t)\geq 0$, $t\in[0,\frac{1}{q_2}]$ under Assumption 3 regarding the initial data, as shown in Lemma 1, the property 1 is thus obtained.
2) Consider a Lyapunov function $V(t)=Z(t)^TPZ(t)+\frac{r}{2}\sum_{i=1}^m h_i(t)^2+\frac{1}{2}\int_0^1 e^{-x}\alpha(x,t)^2dx+\frac{1}{2}\int_0^1 a_0e^x\beta(x,t)^2dx$ where the positive-definite matrix $P=P^T$ is the solution to the Lyapunov equation $A_Z^TP+PA_Z=-Q$ for some $Q=Q^T>0$, and where positive constants a_0,r satisfy $a_0\geq\frac{q_1q^2}{q_2}+\frac{4|PB|^2}{q_2\lambda_{\min}(Q)}$, $r>\frac{1}{3}q_2a_0e+1$. Taking the derivative of the Lyapunov function along the target system (15)–(18), (23)–(25), applying Young's inequality, recalling the conditions of the design parameters c_i in (28), we arrive at $\dot V\leq-\sigma_0V(t)$ for some positive σ_0, which shows the exponential stability of the target system. According to the backstepping transformations and their inverses in this section, recalling Assumption 1, we thus obtain the property 2.
3) The property 3 can then be obtained from the property 2. Due to the space limit, we only provide the proof sketch here. Please see the proof of [30, Theorem 1] for the details. □

IV. Output-Positive Adaptive Control Design

A. Adaptive Controller

1) Certainty Equivalence Control Law: First, we build a certainty equivalence adaptive controller, which is potentially unsafe, by replacing the unknown parameters θ in the nominal control input U with the parameter estimate $\hat\theta$, i.e.,

$$U_d(t):=\mathcal{U}(\chi(t);\hat\theta(t_i)),\quad t\in[t_i,t_{i+1}) \tag{30}$$

where $\hat\theta(t_i)=[\hat d_1,\hat d_2,\hat b]^T$, an estimate generated with a triggered batch least-squares identifier that is updated along a sequence of time instants t_i and uses the plant states in a time interval before t_i to produce the parameter estimates, will be defined in Section IV-A2, and where the sequence of triggering time instants $\{t_i\geq 0\}_{i=0}^{\infty}$ is defined as

$$t_{i+1}=t_i+T \tag{31}$$

where T, a positive design parameter, is free. Here, we use the simple triggering mechanism (31) for easier implementation. A more complicated but more effective event-triggering mechanism in [29] to update batch least-squares identifier for hyperbolic PDEs by evaluating the net increase of the system norms can also be used here.

2) Batch Least-Squares Identifier: According to (2), (3), we get for $\tau>0$ and $\bar n=1,2,\cdots$ that

$$\begin{aligned}&\frac{d}{d\tau}\left(\int_0^1\sin(x\pi\bar n)z(x,\tau)dx+\int_0^1\sin(x\pi\bar n)w(x,\tau)dx\right)\\&=-q_2\pi\bar n\int_0^1\cos(x\pi\bar n)w(x,\tau)dx\\&\quad+d_1\int_0^1\sin(x\pi\bar n)w(x,\tau)dx+q_1\pi\bar n\int_0^1\cos(x\pi\bar n)z(x,\tau)dx\\&\quad+d_2\int_0^1\sin(x\pi\bar n)z(x,\tau)dx\end{aligned} \tag{32}$$

$$\frac{d}{d\tau}y_n(\tau)=\sum_{i=1}^n l_iy_i(\tau)+bw(0,\tau). \tag{33}$$

Define the instant μ_{i+1} as $\mu_{i+1}=\min\{t_g:g\in\{0,\ldots,i\},t_g\geq t_{i+1}-\tilde NT\}$ for $i\in\mathbb{Z}^+$, where the positive integer $\tilde N\geq 1$ is a free design parameter. Integrating (32), (33) from μ_{i+1} to t, yields

$$p_{\bar{n}}(t,\mu_{i+1}) = d_1 g_{\bar{n},1}(t,\mu_{i+1}) + d_2 g_{\bar{n},2}(t,\mu_{i+1}) \tag{34}$$

$$p_{\mathrm{b}}(t,\mu_{i+1}) = b q_{\mathrm{b}}(t,\mu_{i+1}) \tag{35}$$

where $p_{\bar{n}}, g_{\bar{n},1}, g_{\bar{n},2}, p_{\mathrm{b}}, q_{\mathrm{b}}$ are given in [30, (74)–(78)]. Define the function $h_{i,\bar{n}} : \mathbb{R}^3 \to \mathbb{R}_+$ by the formula $h_{i,\bar{n}}(\ell) = \int_{\mu_{i+1}}^{t_{i+1}} [(p_{\bar{n}}(t,\mu_{i+1}) - \ell_1 g_{\bar{n},1}(t,\mu_{i+1}) - \ell_2 g_{\bar{n},2}(t,\mu_{i+1}))^2 + (p_{\mathrm{b}}(t,\mu_{i+1}) - \ell_3 q_{\mathrm{b}}(t,\mu_{i+1}))^2]dt$, for $i \in \mathbb{Z}^+$, where $\ell = [\ell_1,\ell_2,\ell_3]^T$. According to (34), (35), the function $h_{i,\bar{n}}(\ell)$ has a global minimum $h_{i,\bar{n}}(\theta) = 0$. We get from Fermat's theorem (differentiating the functions $h_{i,\bar{n}}(\ell)$ with respect to ℓ_1,ℓ_2,ℓ_3, respectively, and using the fact that the derivatives at the position of the global minimum $(\ell_1,\ell_2,\ell_3) = (d_1,d_2,b)$ are zero) that the following matrix equation hold for every $i \in \mathbb{Z}_+$ and $\bar{n} \in \mathbb{N}$:

$$Z_{\bar{n}}(\mu_{i+1},t_{i+1}) = G_{\bar{n}}(\mu_{i+1},t_{i+1})\theta \tag{36}$$

where $\theta = [d_1,d_2,b]^T$ is a column vector of unknown parameters, and where $Z_{\bar{n}} = [H_{\bar{n},1}, H_{\bar{n},2}, H_3]^T$, $G_{\bar{n}} = [Q_{\bar{n},1}, Q_{\bar{n},2}, 0; Q_{\bar{n},2}, Q_{\bar{n},3}, 0; 0, 0, Q_4]$ with $H_{\bar{n},1}, H_{\bar{n},2}, H_3, Q_{\bar{n},1}, Q_{\bar{n},2}, Q_{\bar{n},3}, Q_4$ given by [30, (82)–(88)]. The parameter estimator (update law) is defined as

$$\hat{\theta}(t_{i+1}) = \operatorname{argmin}\Big\{ |\ell - \hat{\theta}(t_i)|^2 : \ell \in \Theta, \; Z_{\bar{n}}(\mu_{i+1},t_{i+1}) = G_{\bar{n}}(\mu_{i+1},t_{i+1})\ell, \; \bar{n} = 1,2,\cdots \Big\} \tag{37}$$

where $\Theta = \{\ell \in \mathbb{R}^3 : \underline{d}_1 \le \ell_1 \le \bar{d}_1, \underline{d}_2 \le \ell_2 \le \bar{d}_2, 0 < \underline{b} \le b \le \bar{b}\}$.

B. Output-Positive Adaptive Controller

The adaptive controller (30) is potentially unsafe because the mismatch between the parameter estimates and the true values leads to the safety obtained in Theorem 1 is not ensured anymore. Next, we design an output-positive adaptive controller by making use of a QP safety filter to override the adaptive controller U_d (30).

Considering the plant parameters d_1, d_2, b that are considered as unknown in this section, the design parameter conditions (27), (28) in the nominal control design are slightly modified as

$$\kappa_i > \max_{\underline{b} \le \varsigma \le \bar{b}} \breve{\kappa}_i(\varsigma), \;\; i = 1,\ldots,n-1 \tag{38}$$

$$c_i > \max\left\{2, \max_{\vartheta \in \Theta} \check{c}_i(\vartheta)\right\}, i = 1,\ldots,m-1, \; c_m > 1 \tag{39}$$

using the known bounds of the unknown parameters in Assumption 2, where $\breve{\kappa}_i$, $\check{c}_i$ are defined in (27), (29), respectively.

With (38), (39), and Assumption 3, the required positive initialization in Lemmas 2 and 3 is achieved. Like the nominal control design, a sufficient condition to the safety guarantee, i.e., the nonnegativity of the functions h_i, β, z_i, is $h_m(t) \ge 0$ all the time, whose sufficient condition is

$$\dot{h}_m(t;\theta) \ge -\bar{c} h_m(t;\theta) \tag{40}$$

under the positive initialization, where the positive constant $\bar{c}$ is a design parameter satisfying $\bar{c} \ge c_m$. Writing $\theta = [d_1,d_2,b]^T$ after ";" in $h_m(t;\theta)$ emphasizes the fact that now h_m depends on the unknown parameters d_1,d_2,b. Considering the uncertainties, recalling (7), (20), (22), and the adaptive estimate (37), it follows the CBF constraint (40) that a safe region of the adaptive control action is

$$\mathcal{C}(t) = \left\{ u \in \mathbb{R} : u \ge \max_{\vartheta \in D_i} U^*(\chi;\vartheta) \right\}, \; t \in [t_i, t_{i+1}) \tag{41}$$

where the explicit function U^* is

$$U^*(\chi;\theta) = (c_m - \bar{c})h_m + \tau_m - \sum_{i=0}^{m-1} \bar{q}_i z_t^{(i)}(1,t) - M^T Y(t) + \Gamma^{(m)}(t) \tag{42}$$

which is identical to (26) when replacing $\bar{c}$ with c_m. The sets D_i are generated in running BaLSI (37) and given by

$$D_i = \{\ell \in \Theta : Z_{\bar{n}}(\mu_i,t_i) = G_{\bar{n}}(\mu_i,t_i)\ell\} \cap D_{i-1} \tag{43}$$

for $i \in \mathbb{N}$ and $D_0 = \Theta$. It implies that

$$\theta \subseteq D_i \subseteq \Theta, \; i \in \mathbb{Z}^+ \tag{44}$$

recalling (36). Computing $\max_{\vartheta \in D_i} U^*(\chi;\vartheta)$ will not cost too much time because $U^*(\chi;\vartheta)$ is an explicit function of ϑ, and the seeking range D_i would possibly be shrunk as time goes on until it becomes a singleton.

Making use of a QP safety filter to guarantee the adaptive control input stays in the safe region (41), we build the output-positive adaptive controller $U_a(t)$ as

$$U_a = \arg\min_{u \in \mathbb{R}} \{|u - U_d|^2\}, \;\text{s.t.}\; u \in \mathcal{C}(t). \tag{45}$$

Remark 1: Our design encompasses all the essential features of a CBF safety design. The chain structures for the two ODEs, i.e., (15), (24), (25) in the target system, are essentially the high relative-degree CBFs, which were introduced in 2006 [16] for nonovershooting control and were independently discovered in 2016 [23]. Moreover, as is typical with traditional CBFs for ODEs, the PDE state $\beta(x,t)$ in the target system is also required to be ensured nonnegative for the purpose of safety. In addition, the QP safety filter often used in the CBF-based control is (45).

C. Result With Output-Positive Adaptive Control

Defining the difference between $U(t)$ and $U_a(t)$ as

$$\eta(t) = U(t) - U_a(t) \tag{46}$$

inserting U_a defined by (30) into (7), recalling the nominal control design in Section III-C, the target system becomes (15)–(18), (23), (24) together with

$$\dot{h}_m(t) = -c_m h_m(t) - \eta(t). \tag{47}$$

Proposition 1: For every $(z[0], w[0], X(0), Y(0)) \in C^{m-1}([0,1])^2 \times \mathbb{R}^m \times \mathbb{R}^n$, there exists a unique solution $(z,w,X,Y) \in C^{m-1}([0,\infty) \times [0,1])^2 \times \mathbb{C}^0([0,\infty);\mathbb{R}^m) \times \mathbb{C}^0([0,\infty);\mathbb{R}^n)$ to the system (1)–(7) with the control input (45).

Proof: Please see the proof of [30, Proposition 1]. □

Lemma 4: The finite-time exact identification of the unknown parameters is achieved, that is, there exists a finite updating time t_f, $f \in \mathbb{Z}^+$, such that $\hat{\theta}(t) \equiv \theta$, $\forall t \ge t_f$. Also, the set D_i defined by (43) is shrunk to a singleton at t_f and is kept at the singleton, which is nothing else but the unknown parameter's true value θ, for $i \ge f$, $i \in \mathbb{Z}^+$.

Proof: The proof is given in [30, Appendix D]. □

Some tips on implementation of the control law (45) to avoid falling into the extreme and rare cases that hinder the finite time exact parameter identification are given in [30, Remark 2]. It follows from Lemma 4 and (31) that the convergence time t_f depends on the plant's initial values and can be influenced by the design parameter T that is a free positive design parameter related to the amount of the measurement data used in parameter estimation.

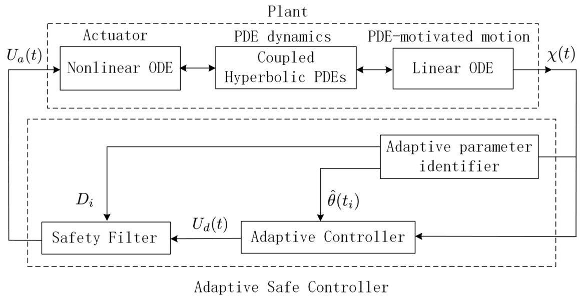

Fig. 1. Diagram of the proposed control system.

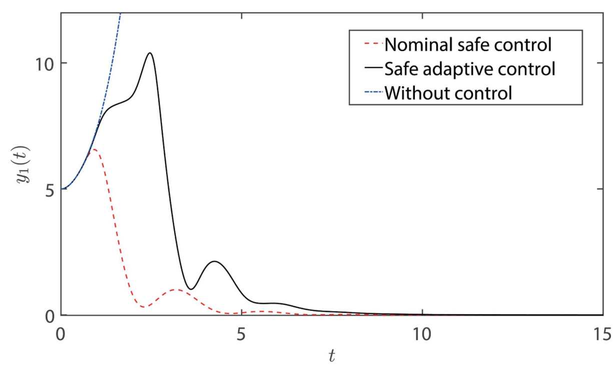

Fig. 2. Responses of the state to be safely regulated (the safe region is the one above the zero line).

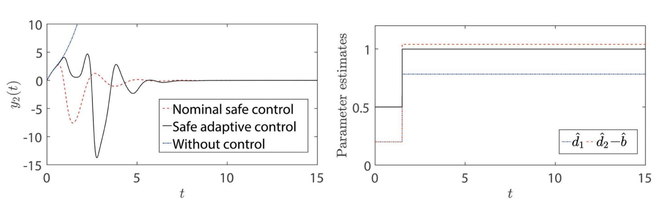

(a) (b)

Fig. 3. Responses of $y_2(t)$ and the parameter estimates. (a) $y_2(t)$. (b) Estimates.

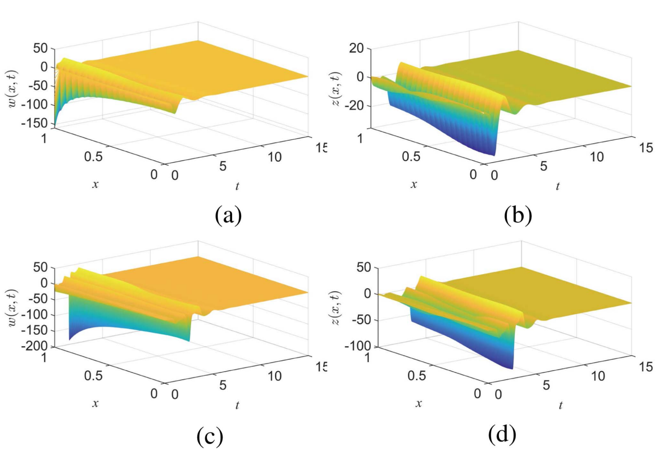

(a) (b)

(c) (d)

Fig. 4. Responses of $w(x,t), z(x,t)$ under the nominal safe and safe adaptive controllers. (a) Nominal safe control. (b) Nominal safe control. (c) Safe adaptive control. (d) Safe adaptive control.

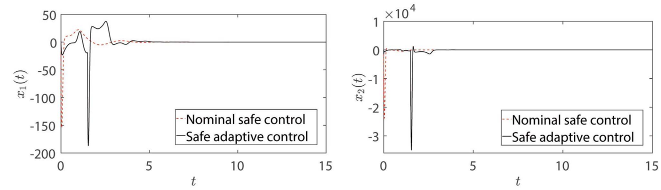

(a) (b)

Fig. 5. Responses of $x_1(t), x_2(t)$ under the nominal safe and safe adaptive controllers. (a) $x_1(t)$. (b) $x_2(t)$.

The result of the output-positive adaptive closed-loop system, whose diagram is shown in Fig. 1, is given as follows.

Theorem 2: For initial data $(w[0], z[0])^T \in C^{m-1}([0,1])$, $\hat{\theta}(0) \in \Theta$, $X(0) \in \mathbb{R}^m$, $Y(0) \in \mathbb{R}^m$ satisfying Assumptions 1–4, for design parameters c_i, $i = 1, \ldots, m$ satisfying (39) and κ_i, $i = 1, \ldots, n-1$ satisfying (38), the closed-loop system including the plant (1)–(7) with the output-positive adaptive controller (45) has the following properties.

1) Safety (output positivity) is ensured in the sense that $y_1(t) \geq 0$, $\forall t \geq 0$. Moreover, it runs in the original safe set like the nominal safe control after the finite time.
2) Exponential regulation of the plant states is achieved in the sense that $\|w(\cdot,t)\|^2 + \|z(\cdot,t)\|^2 + |X(t)|^2 + |Y(t)|^2$ is exponentially convergent to zero.
3) The output-positive adaptive control input is exponentially convergent to zero, i.e., $\lim_{t\to\infty} U_a(t) = 0$.

Proof: 1) According to (41)–(44), the controller (45) with the adaptive CBF constraint guarantees $\dot{h}_m(t) = -\bar{c}h_m(t) + \bar{\eta}(t)$ where $\bar{\eta}(t) = U_a(t) - U^*(\chi;\theta) \geq 0$ because of $U_a \geq \max_{\vartheta\in D_i} U^*(\chi;\vartheta) \geq U^*(\chi;\theta)$ due to (44). It implies that $h_m(t) \geq \bar{\eta}(t) \geq 0$ all the time recalling $h_m(0) > 0$ ensured by the choices of design parameters (39). Especially, for $t \in [t_f, \infty)$, it follows from Lemma 4 that $U_d(t) = U(t)$ recalling the nominal controller $U(t)$ (26) and the adaptive controller U_d (30), as well as the control input's safe region boundary $\max_{\vartheta\in D_i} U^*(\chi;\vartheta) = U^*(\chi;\theta)$ in (42). Then, we have $\max_{\vartheta\in D_i} U^*(\chi;\vartheta) - U_d(t) = U^*(\chi;\theta) - U(t) = (c_m - \bar{c})h_m(t) \leq 0$ for $t \geq t_f$ recalling $\bar{c} \geq c_m$ and $h_m(t) \geq 0$ proven previously. It implies that $U_d \in \mathcal{C}$ because of (41), and thus $U_a = U_d = U$ for $t \geq t_f$ according to (45), which means that $\eta(t) \equiv 0$, $\forall t \geq t_f$ in (47) because of (46). Therefore, $\dot{h}_m(t) = -c_m h_m(t)$ holds on $t \in [t_f, \infty)$, i.e., the state runs in the original safe set like the nominal safe control when $t \geq t_f$. The property 1in this theorem is obtained. Applying $\eta(t) \equiv 0, \forall t \geq t_f$ in (47), the property 2 is obtained following the proof of the property 2 in Theorem 1. 3) The property 3 is straightforwardly obtained from the property 2. □

V. Simulation

A. Model and Controller

The considered simulation model is (1)–(7) with the parameters $A = [0,1;l_1,l_2] = [0,1;1,-0.5]$, $B = [0,b]^T = [0,1]^T$, $q_1 = q_2 = 1$, $d_1 = 0.8$, $d_2 = 1$, $m = 2$, $n = 2$, $p = 1$, $\bar{q}_0 = 1$, $\bar{q}_1 = 1$, $M^T = [0.1, 0.3]$, and the functions f_1 and f_2 in (6), (7) are $f_1(\underline{x}_1) = x_1^2$, $f_2(\underline{x}_2) = x_1 x_2$. The known bounds of the unknown parameters d_1, d_2, b are set as $\overline{d}_1 = \overline{d}_2 = 1.2$, $\underline{d}_1 = \underline{d}_2 = 0.2$, $\overline{b} = 1.5$, $\underline{b} = 0.5$. The initial values are defined as $w(x,0) = \cos(2\pi x)$, $z(x,0) = 2\sin(3\pi x)$, $x_1(0) = 1$, $x_2(0) =$

-1, $y_1(0) = 5$, $y_2(0) = 0$, $\hat{d}_1(0) = \hat{d}_2(0) = 0.2$, $\hat{b}(0) = 0.5$. The initial values in the simulation satisfy Assumptions 3 and 4. The simulation model is open-loop unstable, where the unstable sources exist in every subsystem.

Following the control design in Sections III and IV, we obtain the nominal safe and adaptive safe controllers, whose details are given in [30, Sec. V-B], where we choose the design parameters $c_1, c_2, \kappa_1, \kappa_2, \bar{c}, \bar{n}, \tilde{N}, T$ (the nominal controller only requires $c_1, c_2, \kappa_1, \kappa_2$) as follows. The design parameters $c_1 = 38, c_2 = 20, \kappa_1 = 30, \kappa_2 = 10$ are chosen to satisfy the condition (38), (39) with (27), (29), and the arbitrary positive design parameters $\bar{c} = 50, \bar{n} = 1, \tilde{N} = 10, T = 1.5$ are chosen considering the following tradeoff in implementation. Increasing the design parameter $T, \tilde{N}$ will let more measured data take part in estimation, which is helpful to improve the estimation accuracy but will prolong the duration of adaptive learning. The increase of $\bar{n}$ contributes to finding the true values on time at the cost of more computing resources. The adjustment of $\bar{c}$ will affect the adaptive control input's safe region adopted in the QP safety filter. Some tips on implementation of the parameter identifier (37) are given in [30, Sec. V-B].

B. Simulation Result

We conduct the simulation by the finite-difference method with a time step of 0.001 and a space step of 0.002 for the adaptive case, where the relatively small space step is selected to reduce the approximation error of integration in the identifier mentioned previously, for the nominal case a larger space step as 0.05 can be used to save the computation time.

The response of the distal ODE's output state $y_1(t)$ that is expected to be kept in the safe region, i.e., the nonnegativity, the other state $y_2(t)$ in the distal ODE, and the estimates of the unknown plant parameters d_1, d_2, b are shown in Figs. 2 and 3. In Fig. 2, the three results have the same behavior before $t = 1$ s because in this time period no control action reaches the Y-ODE and the responses only depend on the initial values of the plant. As compared to the nominal safe (output-positive) control, even though the mismatch between the parameter estimates and their true values degrades the control performance of the safe (output-positive) adaptive controller before around $t = 2.5$, the response under the safe adaptive control begins to fast converge to zero like the nominal control result after 2.5 s [the adaption time is 1.5 s that can be seen in Fig. 3(b), and the time taken by the updated control actions spreading from $x = 1$ to $x = 0$ is 1 s]. Both nominal safe and safe adaptive controllers can constrain the output state $y_1(t)$ in the safe region, i.e., $y_1(t) \geq 0$, and achieve the exponential convergence to zero of $y_1(t)$, while the state blows up in the open loop since the simulation model is open-loop unstable. We know from Fig. 3(b) that the exact identification of the unknown parameters is achieved at the first triggering time, under the nonzero initial values given in Section V-A. Please note that the tiny difference between the final estimates $\hat{d}_1, \hat{d}_2$ and their true values comes from approximation error of integration. Reducing the space step of the integration in BaLSI contributes to a smaller estimation error, but requires more computational power. It is shown in Figs. 4 and 5 that the PDE plant states $z(x,t), w(x,t)$, and the nonlinear ODE states $x_1(t), x_2(t)$ all converge to zero under the nominal safe and safe adaptive control inputs.

VI. Conclusion and Future Work

In this article, we present an output-positive adaptive control design method for 2×2 hyperbolic PDEs sandwiched between a strict-feedback nonlinear ODE on the actuated side and a linear ODE on the uncontrolled side. The coefficients of the unstable sources in the PDE domain and of the input signal in the distal ODE to be kept safe are unknown. Our contort design guarantees the safety (nonnegativity) of the state furthermost from the control input and the exponential regulation of overall plant states to zero. The numerical simulation illustrates the validity of the proposed control design. In the future work, we will consider the case that $z(1,t)$ and $Y(t)$ are not accessible, and work on improving the robustness of the controller with respect to the external disturbance.

References

[1] I. Abel, D. Steeves, M. Krstic, and M. Jankovic, "Prescribed-time safety design for a chain of integrators," in *Proc. Amer. Control Conf.*, 2022, pp. 4915–4920.

[2] A. D. Ames, X. Xu, J. W. Grizzle, and P. Tabuada, "Control barrier function based quadratic programs for safety critical systems," *IEEE Trans. Autom. Control*, vol. 62, no. 8, pp. 3861–3876, Aug. 2017.

[3] A. D. Ames, S. Coogan, M. Egerstedt, G. Notomista, K. Sreenath, and P. Tabuada, "Control barrier functions: Theory and applications," in *Proc. 18th Eur. Control Conf.*, 2019, pp. 3420–3431.

[4] H. Anfinsen and O. M. Aamo, *Adaptive Control of Hyperbolic PDEs*. Berlin, Germany: Springer, 2019.

[5] Z. Cao, Y. Yang, J. Lu, and F. Gao, "Constrained two dimensional recursive least squares model identification for batch processes," *J. Process Control*, vol. 24, pp. 871–879, 2014.

[6] Z. Cao, Y. Yang, H. Yi, and F. Gao, "Priori knowledge-based online batch-to-batch identification in a closed loop and an application to injection molding," *Ind. Eng. Chem. Res.*, vol. 55, pp. 8818–8829, 2016.

[7] G. Chowdhary and E. Johnson, "Least squares based modification for adaptive control," in *Proc. 49th IEEE Conf. Decis. Control*, 2010, pp. 1767–1772.

[8] M. H. Cohen and C. Belta, "High order robust adaptive control barrier functions and exponentially stabilizing adaptive control Lyapunov functions," in *Proc. IEEE Amer. Control Conf.*, 2022, pp. 2233–2238.

[9] L. Hu, F. D. Meglio, R. Vazquez, and M. Krstic, "Control of homodirectional and general heterodirectional linear coupled hyperbolic PDEs," *IEEE Trans. Autom. Control*, vol. 61, no. 11, pp. 3301–3314, Nov. 2016.

[10] A. Isaly, O. S. Patil, R. G. Sanfelice, and W. E. Dixon, "Adaptive safety with multiple barrier functions using integral concurrent learning," in *Proc. Amer. Control Conf.*, 2021, pp. 3719–3724.

[11] I. Karafyllis and M. Krstic, "Adaptive certainty-equivalence control with regulation-triggered finite-time least-squares identification," *IEEE Trans. Autom. Control*, vol. 63, no. 10, pp. 3261–3275, Oct. 2018.

[12] I. Karafyllis, M. Krstic, and K. Chrysafi, "Adaptive boundary control of constant-parameter reaction-diffusion PDEs using regulation-triggered finite-time identification," *Automatica*, vol. 103, pp. 166–179, 2019.

[13] S. Koga, C. Demir, and M. Krstic, "Event-triggered safe stabilizing boundary control for the stefan PDE system with actuator dynamics," in *Proc. Amer. Control Conf.*, pp. 1794–1799, 2023.

[14] S. Koga and M. Krstic, "Safe PDE backstepping QP control with high relative degree CBFs: Stefan model with actuator dynamics," *IEEE Trans. Autom. Control*, vol. 68, no. 12, pp. 7195–7208, Dec. 2023, doi: 10.1109/TAC.2023.3250514.

[15] M. Krstic, "On using least-squares updates without regressor filtering in identification and adaptive control of nonlinear systems," *Automatica*, vol. 45, pp. 731–735, 2009.

[16] M. Krstic and M. Bement, "Nonovershooting control of strict-feedback nonlinear systems," *IEEE Trans. Autom. Control*, vol. 51, no. 12, pp. 1938–1943, Dec. 2006.

[17] M. Krstic and P. V. Kokotovic, "Control Lyapunov functions for adaptive nonlinear stabilization," *Syst. Control Lett.*, vol. 26, no. 1, pp. 17–23, 1995.

[18] W. Li and M. Krstic, "Mean-nonovershooting control of stochastic nonlinear systems," *IEEE Trans. Autom. Control*, vol. 66, no. 12, pp. 5756–5771, Dec. 2021.

[19] B. T. Lopez, J. E. Slotine, and J. P. How, "Robust adaptive control barrier functions: An adaptive and data-driven approach to safety," *IEEE Control Syst. Lett.*, vol. 5, no. 3, pp. 1031–1036, Jul. 2021.

[20] B. T. Lopez and J. E. Slotine, "Unmatched control barrier functions: Certainty equivalence adaptive safety," in *Proc. Amer. Control Conf.*, 2023, pp. 3662–3668.

[21] M. Maghenem, A. J. Taylor, A. D. Ames, and R. G. Sanfelice, “Adaptive safety using control barrier functions and hybrid adaptation,” in *Proc. Amer. Control Conf.*, 2021, pp. 2418–2423.
[22] F. D. Meglio, F. Bribiesca-Argomedo, L. Hu, and M. Krstic, “Stabilization of coupled linear heterodirectional hyperbolic PDE-ODE systems,” *Automatica*, vol. 87, pp. 281–289, 2018.
[23] Q. Nguyen and K. Sreenath, “Exponential control barrier functions for enforcing high relative-degree safety-critical constraints,” in *Proc. Amer. Control Conf.*, 2016, pp. 322–328.
[24] A. Smyshlyaev and M. Krstic, *Adaptive Control of Parabolic PDEs*. Princeton, NJ, USA: Princeton Univ. Press, 2010.
[25] A. J. Taylor and A. D. Ames, “Adaptive safety with control barrier functions,” in *Proc. Amer. Control Conf.*, 2020, pp. 1399–1405.
[26] K. P. Tee, S. S. Ge, and E. H. Tay, “Barrier Lyapunov functions for the control of output-constrained nonlinear systems,” *Automatica*, vol. 45, no. 4, pp. 918–927, 2009.
[27] R. Vazquez, M. Krstic, and J. M. Coron, “Backstepping boundary stabilization and state estimation of a 2×2 linear hyperbolic system,” in *Proc. 50th Conf. Decis. Control Eur. Control Conf.*, 2011, pp. 4937–4942.
[28] J. Wang and M. Krstic, “Regulation-triggered adaptive control of a hyperbolic PDE-ODE model with boundary interconnections,” *Int. J. Adaptive Control Signal Process*, vol. 35, no. 8, pp. 1513–1543, 2021.
[29] J. Wang and M. Krstic, “Event-triggered adaptive control of coupled hyperbolic PDEs with piecewise-constant inputs and identification,” *IEEE Trans. Autom. Control*, vol. 68, no. 3, pp. 1568–1583, Mar. 2023.
[30] J. Wang and M. Krstic, “Output-positive adaptive control of hyperbolic PDE-ODE cascades,” 2024, *arXiv:2309.05596v3*.
[31] Z. Wang and D. R. Liu, “Data-based output feedback control using least squares estimation method for a class of nonlinear systems,” *Int. J. Robust Nonlinear Control*, vol. 24, pp. 3061–3075, 2014.
[32] Y. Wang and X. Xu, “Adaptive safety-critical control for a class of nonlinear systems with parametric uncertainties: A control barrier function approach,” *Syst. Control Lett.*, vol. 188, p. 105798, 2024.
[33] W. Xiao and C. Belta, “Control barrier functions for systems with high relative degree,” in *Proc. Conf. Decis. Control*, 2019, pp. 474–479.
[34] W. Xiao and C. Belta, “High order control barrier functions,” *IEEE Trans. Autom. Control*, vol. 67, no. 7, pp. 3655–3662, Jul. 2022.
[35] Y. Zhang et al., “Adaptive safe reinforcement learning with full-state constraints and constrained adaptation for autonomous vehicles,” *IEEE Trans. Cybern.*, vol. 54, no. 3, pp. 1907–1920, Mar. 2024.
[36] Y. Zhang et al., “Barrier Lyapunov function-based safe reinforcement learning for autonomous vehicles with optimized backstepping,” *IEEE Trans. Neural Netw. Learn. Syst.*, vol. 35, no. 2, pp. 2066–2080, Feb. 2024.